Molecular Neurobiology (2019) 56:2760–2773
https://doi.org/10.1007/s12035-018-1275-6

Disruption of Brain Redox Homeostasis, Microglia Activation and Neuronal Damage Induced by Intracerebroventricular Administration of S-Adenosylmethionine to Developing Rats

Bianca Seminotti[1] · Ângela Zanatta[1] · Rafael Teixeira Ribeiro[1] · Mateus Struecker da Rosa[1] · Angela T. S. Wyse[1,2] · Guilhian Leipnitz[1,2] · Moacir Wajner[1,2,3]

Received: 18 May 2018 / Accepted: 22 July 2018 / Published online: 30 July 2018

Abstract

S-Adenosylmethionine (AdoMet) concentrations are highly elevated in tissues and biological fluids of patients affected by S-adenosylhomocysteine hydrolase deficiency. This disorder is clinically characterized by severe neurological symptoms, whose pathophysiology is not yet established. Therefore, we investigated the effects of intracerebroventricular administration of AdoMet on redox homeostasis, microglia activation, synaptophysin levels, and TAU phosphorylation in cerebral cortex and striatum of young rats. AdoMet provoked significant lipid and protein oxidation, decreased glutathione concentrations, and altered the activity of important antioxidant enzymes in cerebral cortex and striatum. AdoMet also increased reactive oxygen (2′,7′-dichlorofluorescein oxidation increase) and nitrogen (nitrate and nitrite levels increase) species generation in cerebral cortex. Furthermore, the antioxidants N-acetylcysteine and melatonin prevented most of AdoMet-induced pro-oxidant effects in both cerebral structures. Finally, we verified that AdoMet produced microglia activation by increasing Iba1 staining and TAU phosphorylation, as well as reduced synaptophysin levels in cerebral cortex. Taken together, it is presumed that impairment of redox homeostasis possibly associated with microglia activation and neuronal dysfunction caused by AdoMet may represent deleterious pathomechanisms involved in the pathophysiology of brain damage in S-adenosylhomocysteine hydrolase deficiency.

Keywords S-Adenosylhomocysteine hydrolase deficiency · S-Adenosylmethionine · Redox homeostasis · Microglia activation · Neuronal damage

Introduction

Deficiency of the activity of the enzyme S-adenosylhomocysteine (AdoHcy) hydrolase (EC 3.3.1.1) that catalyzes the reaction AdoHcy to adenosine (Ade) and homocysteine is a rare inborn error of metabolism first described by Gaull and colleagues [1] in a patient presenting with psychomotor development delay, white matter atrophy with hypomyelination, marked hypotonia, and liver dysfunction. Biochemical findings in this patient were hypermethioninemia and highly increased blood concentrations of S-adenosylmethionine (AdoMet) and AdoHcy. So far, a total of 10 patients from six families have been reported in the literature, with predominant psychomotor and developmental delay, epilepsy, myopathy, hepatopathy, coagulation defects, microcephaly, and hypomyelination, as well as a high tissue accumulation of methionine (Met), AdoMet, and AdoHcy. Symptomatology is commonly observed in early stages of life, mainly during childhood [2–6]. Treatment with a low-methionine diet, associated with creatine and phosphatidylcholine supplementation, is often ineffective [7].

The pathophysiology of the neurological symptoms observed in AdoHcy hydrolase deficiency is not yet established. However, it is emphasized that AdoHcy is critical for the regulation of the transsulfuration-transmethylation cycle involving methionine supply and methyl group distribution

✉ Moacir Wajner
mwajner@ufrgs.br

[1] Programa de Pós-Graduação em Ciências Biológicas: Bioquímica, Instituto de Ciências Básicas da Saúde, Universidade Federal do Rio Grande do Sul, Porto Alegre, RS, Brazil

[2] Departamento de Bioquímica, Instituto de Ciências Básicas da Saúde, Universidade Federal do Rio Grande do Sul, Rua Ramiro Barcelos, 2600-Anexo, Porto Alegre, RS CEP 90035-003, Brazil

[3] Serviço de Genética Médica, Hospital de Clínicas de Porto Alegre, Porto Alegre, RS, Brazil

[7–10]. Furthermore, AdoMet, as a major methyl donor, influences cellular transmethylation pathways in the central nervous system, such as the methylation of DNA, histones, protein phosphatase 2A, and several catecholamine moieties [11]. Therefore, high levels of AdoMet may deregulate cellular methylation altering several AdoMet-dependent reactions and change neurotransmitter concentrations that are critical to the brain functioning [7, 12, 13]. Furthermore, Ade depletion due to inadequate cleavage of AdoHcy may reduce glutathione (GSH) concentrations due to impaired conversion of Met to cysteine, the metabolic precursor of GSH, disturbing cell redox status. In this context, it should be highlighted that the brain is highly susceptible to free radical attack due to its low antioxidant defenses and high oxygen consumption potentially leading to a high production of reactive oxygen species (ROS) [14]. In line with these observations, a recent work demonstrated that AdoMet induces oxidative stress in vitro in rat brain, as determined by lipid and protein damage, and decreased GSH concentrations, apart from reducing Na^+,K^+-ATPase activity that is necessary for neurotransmission [15].

The purpose of the present study was to investigate the effect of intracerebral AdoMet administration on a large spectrum of redox homeostasis parameters, namely malondialdehyde (MDA) levels, carbonyl formation, sulfhydryl oxidation, GSH levels, 2′,7′-dichlorofluorescein (DCFH) oxidation, and nitric oxide production in cerebral cortex and striatum of young rats. Microglia activation, determined by Iba1 staining, TAU phosphorylation, and synaptophysin levels, were also evaluated. Finally, we tested whether potent antioxidants, such as melatonin and N-acetylcysteine, could prevent some of the deleterious effects of AdoMet on cell redox status.

Material and Methods

Chemicals

All chemicals were of analytical grade and purchased from Sigma (St. Louis, MO, USA) unless otherwise stated. AdoMet and NaCl (0.9%) solutions were prepared on the same day of the experiments and had their pH adjusted to 7.4 with NaOH.

Animals

Thirty-day-old Wistar rats were obtained from the Central Animal House of the Department of Biochemistry, ICBS, Universidade Federal do Rio Grande do Sul, Porto Alegre, RS, Brazil. The animals were maintained on a 12:12-h light/dark cycle (lights on 07:00–19:00 h) in air-conditioned constant temperature (22 ± 1 °C) colony room, with free access to water and a 20% (*w*/*w*) protein commercial chow (SUPRA, Porto Alegre, RS, Brazil). The experimental protocol was approved by the local Animal Ethics Committe of Universidade Federal do Rio Grande do Sul. The guidelines of National Institutes of Health Guide for the Care and Use of Laboratory Animals (NIH publication no. 80–23, revised 2011) and Directive 2010/63/EU were followed. All efforts were made to minimize the number of animals used and their suffering.

AdoMet and NaCl Administration

Thirty-day-old rats were used because animals of this age correspond to the period of life in which symptomatology is clearly seen in the affected patients. The animals were deeply anesthetized intraperitoneally with a mixture of ketamine (90 mg/kg) and xylazine (60 mg/kg), and thereafter placed in a stereotaxic apparatus. Two small holes were drilled in the skull, and 2 μL of a 1.0 M AdoMet (2 μmol in a final volume of 2 μL) or 0.9% NaCl (control) at the same volume was slowly injected bilaterally over 2 min into each lateral ventricle via a needle connected by a polyethylene tube to a 10-μL Hamilton syringe. The needle was left in place for a further 1 min before being gently removed. The coordinates for injection were as follows: 0.6 mm posterior to the bregma, 1.1 mm lateral to the midline, and 3.2 mm ventral from dura [16]. The animals were euthanized 2 h, 24 h, or 5 days after AdoMet injection for evaluation of redox homeostasis parameters, protein levels by western blot, and immunohistochemistry, respectively.

Melatonin and N-Acetylcysteine Administration

In some experiments, 27-day-old rats were pretreated intraperitoneally with melatonin (MEL; 20 mg/kg) or N-acetylcysteine (NAC; 150 mg/kg) once a day for 3 days. At 30 days of age, the animals received a further administration of the antioxidants 60 min before the intracerebral injection of AdoMet [17].

Tissue Brain Preparation

Cerebral cortex and striatum were homogenized in 4 (*w*/*v*) (measurement of nitrate and nitrite content) or 10 volumes (*w*/*v*) (determination of MDA and GSH levels, carbonyl formation, sulfhydryl content, antioxidant enzymes activities, and DCFH oxidation) of 20 mM sodium phosphate buffer, pH 7.4, containing 140 mM KCl. Homogenates were centrifuged at 750×*g* for 10 min at 4 °C [18]. The pellet was discarded and the supernatant containing mitochondria and other cell organelles was used to measure the biochemical parameters. Protein content was quantified for data normalization according to Lowry et al. [19].

Biomolecule Oxidative Damage

Lipid peroxidation was estimated by measuring MDA levels according to the method described by Yagi [20] with slight modifications. One hundred microliters of tissue supernatants was treated with 200 μL of 10% trichloroacetic acid (TCA) and 300 μL of 0.67% thiobarbituric acid in 7.1% sodium sulfate and incubated for 2 h in a boiling water bath. After cooling, the mixture was extracted with 400 μL of butanol. Fluorescence of the organic phase was read at 515 and 553 nm as excitation and emission wavelengths, respectively. A calibration curve was performed using 1,1,3,3-tetramethoxypropane and subjected to the same treatment as supernatants. MDA levels were expressed as nmol MDA/mg protein.

Protein oxidation was determined by carbonyl formation and sulfhydryl content. Carbonyl formation was measured by a spectrophotometric assay according to Reznick and Packer [21]. Two hundred microliters of supernatants was treated with 400 μL of 10 mM 2,4-dinitrophenylhydrazine (DNPH) dissolved in 2.5 N HCl or with 2.5 N HCl (blank) and left in the dark for 1 h. The proteins present in the samples were then precipitated with 600 μL of 20% TCA and centrifuged for 5 min at 10,000×*g*. The pellet was washed with 1 mL of ethanol:ethyl acetate (1:1, *v*/*v*) to remove the excess of DNPH and suspended in 550 μL of 6 M guanidine prepared in 2.5 N HCl. The difference between the DNPH-treated and HCl-treated samples (blank) was used to calculate the carbonyl content determined at 365 nm. The results were calculated as nmol carbonyl groups/mg protein, using the extinction coefficient of $22{,}000 \times 10^6$ nmol/mL for aliphatic hydrazones.

Sulfhydryl content was measured based on the reduction of 5,5-dithio-bis (2-nitrobenzoic acid) (DTNB) by thiols, generating a yellow derivative (TNB) whose absorption is measured spectrophotometrically at 412 nm [22]. Briefly, 30 μL of 10 mM DTNB and 980 μL of PBS were added to 50 μL of tissue supernatants. This was followed by a 30-min incubation at room temperature in a dark room. Absorption was measured at 412 nm. The results were calculated and expressed as nmol thiol/mg protein.

Antioxidant Defenses

Nonenzymatic antioxidant defenses were determined by measuring reduced glutathione (GSH), total glutathione (tGS), and oxidized glutathione (GSSG) concentrations. GSH concentrations were measured according to Browne and Armstrong [23]. One hundred eighty-five microliters of 100 mM sodium phosphate buffer, pH 8.0, containing 5 mM EDTA, and 15 μL of *o*-phthaldialdehyde (1 mg/mL) were added to 30 μL of sample (0.3–0.5 mg of protein) previously deproteinized with metaphosphoric acid. After incubating this mixture at 25 °C in a dark room for 15 min, the fluorescence was measured using excitation and emission wavelengths of 350 and 420 nm, respectively. A calibration curve was prepared with standard GSH (0.001–1 mM) and the concentrations were calculated as nmol GSH/mg protein.

tGS and GSSG concentrations were determined by following the enzymatic recycling method described by Teare et al. [24]. Briefly, cerebral cortex and striatum were homogenized in 4 volumes (*w*/*v*) of a mixture (1:1) of 11% sulfosalicylic acid and 0.11% Triton X-100. After a 5-min incubation at 4 °C under continuous shaking, the samples were centrifuged at 10,000×*g* for 10 min at 4 °C. The supernatant was collected for analysis of glutathione levels. For GSSG measurement, 10 μL of this supernatant was added to 110 μL of a GSH masking buffer (100 mM phosphate buffer, 1 mM EDTA, 1.1% 2-vinylpyridine), pH 7.4, and incubated for 1 h at room temperature. The samples prepared for tGS and GSSG quantification were then subjected to enzymatic recycling analysis in a recycling buffer system consisting of 300 μM NADPH, 225 μM DTNB, 1.6 U/mL glutathione reductase (GR), and 1.0 mM EDTA in 100 mM phosphate buffer, pH 7.4. The linear increase in absorbance at 405 nm over time was monitored using a microplate reader (Spectramax M5, Molecular Devices, CA, USA). A standard curve was built with known amounts of GSH (100 mM) and GSSG (3.47, 6.95, and 13.9 mM).

The activities of the following antioxidant enzymes were also measured: glutathione peroxidase (GPx), GR, superoxide dismutase (SOD), catalase (CAT), glucose-6-phosphate dehydrogenase (G6PDH), and glutathione S-transferase (GST). The specific activity was calculated and expressed as U/mg protein.

GPx activity was measured according to Wendel [25] using tert-butyl hydroperoxide as substrate. The enzyme activity was determined by monitoring the NADPH disappearance at 340 nm in a medium containing 100 mM potassium phosphate buffer/1 mM EDTA, pH 7.7, 2 mM GSH, 0.1 U/mL GR, 0.4 mM azide, 0.5 mM tert-butyl hydroperoxide, 0.1 mM NADPH, and tissue supernatants.

GR activity was measured according to Carlberg and Mannervik [26] using GSSG and NADPH as substrates. The enzyme activity was determined by monitoring the NADPH disappearance at 340 nm in a medium with 200 mM sodium phosphate buffer, pH 7.5, containing 6.3 mM EDTA, 1 mM GSSG, 0.1 mM NADPH, and tissue supernatants.

SOD activity was assayed according to Marklund [27] and is based on the capacity of pyrogallol to autooxidize, a process highly dependent on superoxide, which is a substrate for SOD. The inhibition of autoxidation of pyrogallol occurs in the presence of SOD, whose activity can be then indirectly assayed spectrophotometrically at 420 nm. The reaction medium contained 50 mM Tris buffer/1 mM EDTA, pH 8.2, 80 U/mL CAT, 0.38 mM pyrogallol, and tissue supernatants.

CAT activity was assayed according to Aebi [28] by measuring the absorbance decrease at 240 nm in a reaction

medium containing 20 mM H_2O_2, 0.1% Triton X-100, 10 mM potassium phosphate buffer, pH 7.0, and tissue supernatants.

GST activity was measured according to Guthenberg and Mannervik [29] with slight modifications. GST activity was determined by the rate of formation of dinitrophenyl-S-glutathione at 340 nm in a medium containing 50 mM potassium phosphate, pH 6.5, 1 mM GSH, 1 mM 1-chloro-2,4-dinitrobenzene (CDNB) as substrate, and tissue supernatants.

G6PDH activity was measured by the method of Leong and Clark [30] in a reaction mixture containing 100 mM Tris-HCl, pH 7.5, 10 mM $MgCl_2$, 0.5 mM $NADP^+$, and tissue supernatants. The reaction was started by the addition of 1 mM glucose-6-phosphate and was followed in a spectrophotometer at 340 nm.

Reactive Species Formation

Reactive oxygen and nitrogen species production was also quantified in cerebral cortex and striatum supernatants.

ROS production was assessed according to LeBel et al. [31] by using 2′,7′-dihydrodichlorofluorescein diacetate (DCF-DA). DCF-DA (5 μM) was prepared in 20 mM sodium phosphate buffer, pH 7.4, containing 140 mM KCl and incubated with tissue supernatants during 60 min at 37 °C. DCF-DA is enzymatically hydrolyzed by intracellular esterases to form non-fluorescent DCFH, which is then rapidly oxidized to form highly fluorescent 2′,7′-dichlorofluorescein (DCF) in the presence of ROS. Fluorescence was measured using excitation and emission wavelengths of 480 and 535 nm, respectively. A calibration curve was prepared with DCF (0.25–10 mM). The levels of ROS were calculated and expressed as pmol DCF/mg protein.

Nitrate and nitrite concentrations were evaluated according to Navarro-Gonzálvez et al. [32]. One hundred fifty microliters of tissue supernatants was deproteinized by adding 125 μL of 75 mM $ZnSO_4$ solution, followed by centrifugation at 9000×*g* for 2 min at 25 °C. The supernatant obtained was neutralized with 55 mM NaOH solution and diluted in 5 volumes of glycine buffer, pH 9.7. Copper-coated cadmium granules (600–1000 mg) were added to the supernatants to convert all nitrates into nitrite in the biological samples. Aliquots of 200 μL were then treated with 200 μL of Griess reagent (2% sulfanilamide in 5% HCl and 0.1% N-1-(naphthyl)ethylenediamine in H_2O) and incubated at room temperature by 10 min. The absorbance was read at 505 nm. A calibration curve was prepared with $NaNO_2$ at concentrations ranging from 1 to 125 μM. The final results were calculated and expressed as μmol nitrate and nitrite/mg protein.

Immunohistochemical Analysis

Animals were anesthetized with an intraperitoneal injection of a mixture of ketamine (80 mg kg^{-1}) and xylazine (10 mg kg^{-1}) until complete unresponsiveness to nociceptive stimuli and thereafter injected with AdoMet or NaCl solutions. Five days afterwards, they were transcardially perfused with 0.4% sodium citrate prepared in 0.9% saline, and 4% paraformaldehyde (PFA) prepared in 0.1 M phosphate buffer, pH 7.4, to fix the brain. Fixed brains were removed, post-fixed by immersion in PFA during 24 h, and then sectioned on a vibrating microtome to obtain 40-μm-thick consecutive coronal series. Immunohistochemistry was performed using transverse cerebral sections of neocortex and striatum of rats euthanized 5 days after AdoMet or NaCl administration, according to Moura et al. [33]. For each animal and staining procedure, three to six equivalent sections were immunostained. Slices were incubated with the antibody anti-Iba1 (1:300, Wako Co.) diluted in PBST (phosphate-buffered saline with Tween-20). After a 4 °C overnight incubation, sections were rinsed in PBS and incubated at room temperature for 2 h with a secondary antibody (1:500) conjugated to fluorescent probes (Molecular Probes). Sections were then washed, mounted using fluoroshield (Sigma-Aldrich Co.), and imaged in a FV300 Olympus confocal microscope provided with 488 and 546 nm lasers. Primary or secondary antibodies were omitted in negative controls [33].

Preparation of Samples for Western Blot Analysis

The rats were euthanized by decapitation without anesthesia 24 h after AdoMet or NaCl injection and had their brain rapidly excised on a Petri dish placed on ice. Striatum and cerebral cortex were homogenized in a RIPA buffer containing protease and phosphatase inhibitors (1 mM sodium orthovanadate, 1 mM aprotinin, and 1% protease inhibitor cocktail) and centrifuged at 10,000×*g* for 10 min at 4 °C. Supernatant protein concentrations were determined by the method of Lowry et al. [19], then denaturated in 4× Laemmli buffer (250 mM Tris, 8% SDS, 40% glycerol, and 0.002% bromophenol blue, pH 6.7) and 10% 2-mercaptoethanol. These samples were then heated at 98 °C for 5 min and equal amounts of protein (30 μg/well) were fractionated by SDS-PAGE and electroblotted onto nitrocellulose membranes. After verifying protein loading and electroblotting efficiency through Ponceau S staining, the membrane was blocked in Tween-Tris-buffered saline (TTBS: 100 mM Tris-HCl, pH 7.5, 0.9% NaCl, and 0.1% Tween-20) containing 5% albumin. Membranes were then incubated overnight at 4 °C with the primary antibodies anti-heme oxygenase-1 (Abcam® ab13248), anti-synaptophysin (Abcam® ab8049), anti-Tau, and anti-phospho-Tau (Cell Signaling Technology® #4019 and #5383, respectively) separately in TTBS, at different working dilutions as suggested by the manufacturers, and finally washed with TTBS. Anti-rabbit or anti-mouse IgG peroxidase-linked secondary antibody (1:10,000; Santa Cruz®, sc-2030 and sc-2031,

respectively) was then incubated with the membranes for an additional 2 h, following by washed again, and the immunoreactivity was detected by enhanced chemiluminescence. Densitometric analysis was performed with ImageJ software. Blots were developed to be linear in the range used for densitometry. All results were expressed as a ratio relative to the β-actin (1:1000, Sigma-Aldrich® A1978) internal control.

Statistical Analysis

Data were analyzed using Student's t test for unpaired samples or one-way analysis of variance (ANOVA) followed by the Tukey multiple range test when the F value was significant, using the GraphPad 6.0 software. Only significant values are shown in the text. Differences between groups were rated significant at $P < 0.05$. All data presented here are the result of three or more independent experiments.

Results

AdoMet Intracerebral Administration Induces Biomolecule Oxidative Damage

We initially evaluated the effects of AdoMet ICV administration on lipid peroxidation by determining MDA levels in cerebral cortex and striatum of rats euthanized 2 h after the injection. We verified that AdoMet increased MDA levels in the cerebral cortex (Fig. 1a) [$t_{(7)} = 4.572$, $P = 0.0026$], but not in the striatum (Fig. 1d). We also measured the effects of AdoMet on carbonyl formation and sulfhydryl content, markers of protein oxidative damage. AdoMet significantly increased carbonyl formation (Fig. 1b, e) [(b): $t_{(3)} = 4.538$, $P = 0.02$; (e): $t_{(9)} = 2.876$, $P = 0.0183$] and decreased sulfhydryl content (Fig. 1c, f) [(c): $t_{(8)} = 3.867$, $P = 0.0048$; (f): $t_{(9)} = 3.554$, $P = 0.0062$] in both cerebral structures.

AdoMet Intracerebral Administration Decreases tGS and GSH and Increases GSSG Concentrations

tGS, GSH, and GSSG concentrations, which reflect the non-enzymatic antioxidant defenses, were then determined. AdoMet decreased the levels of GSH in cerebral cortex and striatum (Fig. 2a, d) [(a): $t_{(7)} = 4.437$, $P = 0.003$; (d): $t_{(8)} = 4.703$, $P = 0.0015$], as well as of tGS levels, while increased GSSG content in the striatum (Fig. 2e, f) [(e): $t_{(4)} = 4.359$, $P = 0.0121$; (f): $t_{(7)} = 3.072$, $P = 0.018$], but not in the cerebral cortex (Fig. 2b, c).

AdoMet Intracerebral Administration Alters Antioxidant Enzyme Activities

We next determined the effects of AdoMet administration on the activities of important antioxidant enzymes. As shown in Fig. 3, AdoMet decreased the activities of GPx (Fig. 3a, g) [(a): $t_{(8)} = 6.729$, $P = 0.0001$; (g): $t_{(5)} = 5.544$, $P = 0.0026$], GR (Fig. 3b, h) [(b): $t_{(6)} = 2.958$, $P = 0.0256$; (h): $t_{(8)} = 2.996$, $P = 0.0172$], and SOD (Fig. 3c, i) [(c): $t_{(9)} = 4.411$, $P = 0.0017$; (i): $t_{(10)} = 2.619$, $P = 0.0257$] in both cerebral cortex and striatum. We also observed an increase of CAT (Fig. 3d, j) [(d): $t_{(6)} = 3.673$, $P = 0.0104$; (j): $t_{(5)} = 2.976$, $P = 0.0309$] and GST (Fig. 3e, k) [(e): $t_{(6)} = 5.963$, $P = 0.001$; (k): $t_{(7)} = 2.401$, $P = 0.0474$] activities caused by AdoMet in these cerebral regions, while G6PDH activity was increased by this metabolite only in cerebral cortex (Fig. 3f) [(f): $t_{(4)} = 5.134$, $P = 0.0068$].

AdoMet Intracerebral Administration Increases ROS and RNS Generation

ROS generation, assessed by DCFH oxidation, and RNS formation, determined by measurement of nitrate and nitrite content, were also evaluated. Figure 4 displays that DCFH oxidation (Fig. 4a) [(a): $t_{(8)} = 3.609$, $P = 0.0069$] and nitrate and nitrite content (Fig. 4b) [(b): $t_{(8)} = 2.840$, $P = 0.0218$] were significantly increased in the cerebral cortex of AdoMet-injected animals. On the other hand, no alterations were detected in striatum of these animals (Fig. 4c, d).

NAC and MEL Prevent AdoMet-Induced Lipid and Protein Oxidative Damage and the Alterations on the Antioxidant Defenses

Since our data demonstrated that AdoMet disrupts redox homeostasis, we evaluated the influence of the antioxidants NAC and MEL on AdoMet-induced pro-oxidant effects. We observed that both compounds attenuated or prevented most effects induced by AdoMet.

In cerebral cortex, NAC and MEL significantly reduced AdoMet-induced increase of MDA levels (Fig. 5a) [(a): $F_{(3,19)} = 12.82$; $P = 0.0002$] and decrease of GSH concentrations (Fig. 6a) [(a): $F_{(3,14)} = 10.08$, $P = 0.0017$], as well as the alterations of GR (Fig. 6c) [(c): $F_{(3,17)} = 9.468$, $P = 0.0011$], SOD (Fig. 6d) [(d): $F_{(3,17)} = 9.813$, $P = 0.001$], and G6PDH (Fig. 6g) [(g): $F_{(3,18)} = 10.19$, $P = 0.0007$] activities. MEL also prevented sulfhydryl content decrease (Fig. 5b) [(b): $F_{(3,13)} = 31.57$, $P < 0.0001$], while NAC prevented carbonyl formation increase (Fig. 5c) [(c): $F_{(3,19)} = 9.722$, $P = 0.0007$] and the alterations of GPx and GST activities (Fig. 6b, f) [(b): $F_{(3,17)} = 14.95$, $P = 0.0001$; (f): $F_{(3,15)} = 7.057$, $P = 0.0055$] provoked by AdoMet. In contrast, no alterations were seen in DCFH oxidation and CAT activity.

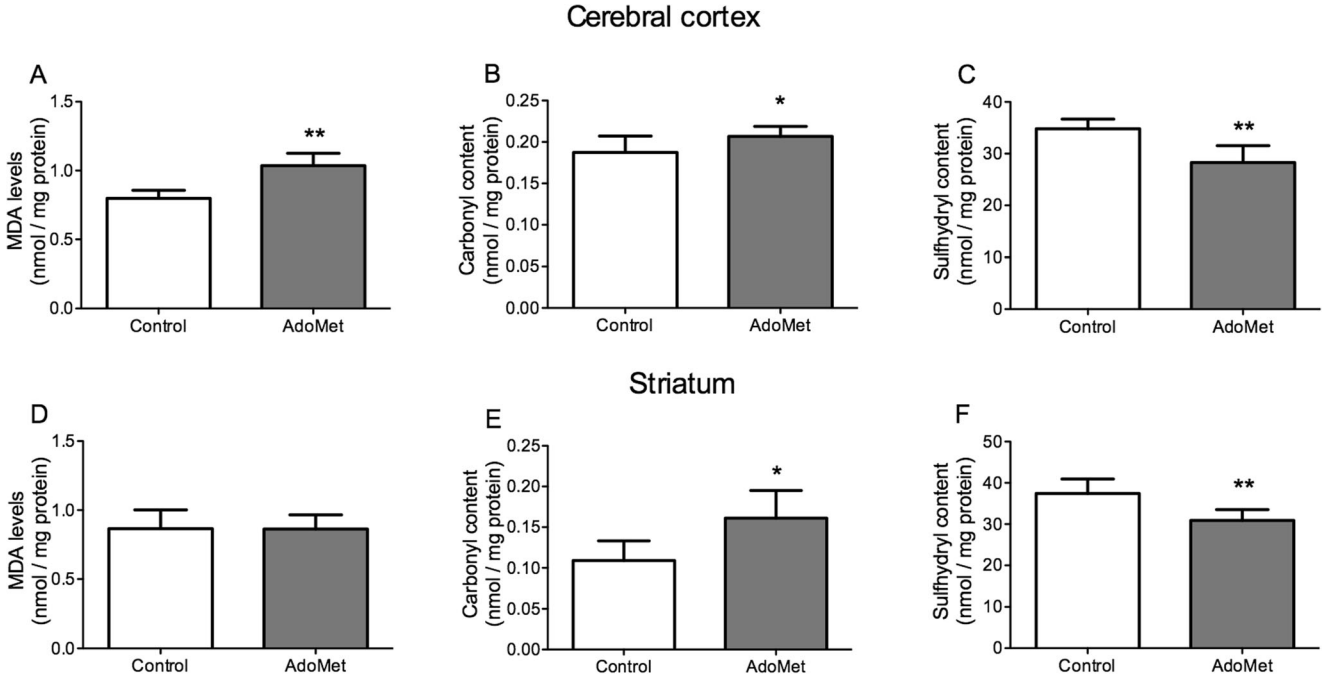

Fig. 1 Effect of S-adenosylmethionine (AdoMet) intracerebroventricular administration on malondialdehyde (MDA) levels (**a**, **d**), carbonyl formation (**b**, **e**), and sulfhydryl content (**c**, **f**) in cerebral cortex and striatum of 30-day-old rats. Animals were euthanized 2 h after AdoMet injection. Data are represented as mean ± SD for 5–6 independent experiments (animals) performed in triplicate. $*P \leq 0.05$, $**P \leq 0.01$, compared to controls (Student's *t* test for unpaired samples)

In striatum, NAC and MEL also exerted protective effects, but to a lesser degree. Thus, NAC and MEL prevented the decrease of GSH levels (Fig. 7b) [(b): $F_{(3,16)} = 10.00$, $P = 0.0072$] and GR activity (Fig. 7d) [(d): $F_{(3,15)} = 6.751$, $P =$

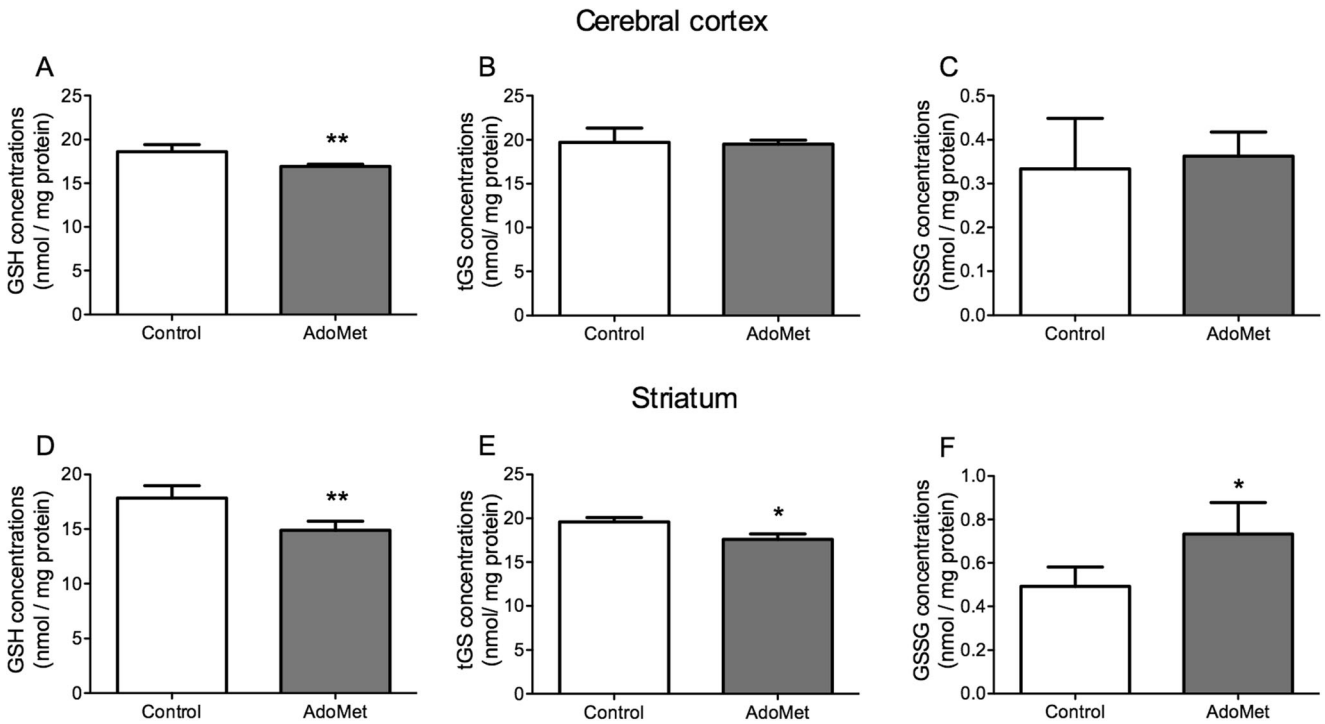

Fig. 2 Effect of S-adenosylmethionine (AdoMet) intracerebroventricular administration on reduced glutathione (GSH; **a**, **d**), total glutathione (tGS; **b**, **e**), and oxidized glutathione (GSSG; **c**, **f**) concentrations in cerebral cortex and striatum of 30-day-old rats. Animals were euthanized 2 h after AdoMet injection. Data are represented as mean ± SD for 5–6 independent experiments (animals) performed in triplicate. $*P \leq 0.05$, $**P \leq 0.01$, compared to controls (Student's *t* test for unpaired samples)

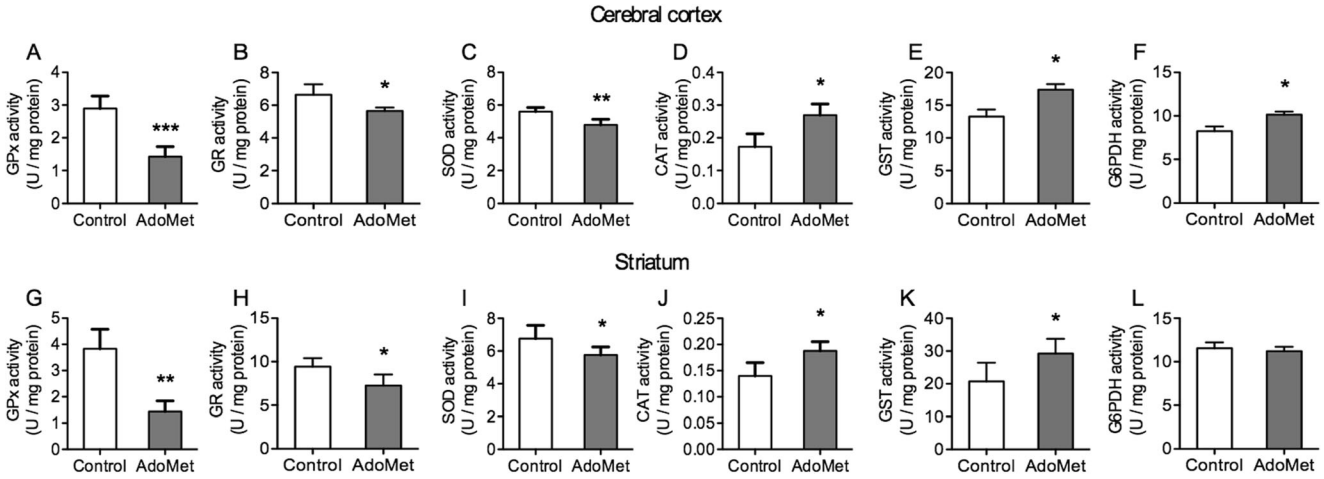

Fig. 3 Effect of S-adenosylmethionine (AdoMet) intracerebroventricular administration on glutathione peroxidase (GPx; **a**, **g**), glutathione reductase (GR; **b**, **h**), superoxide dismutase (SOD; **c**, **i**), catalase (CAT; **d**, **j**), glutathione S-transferase (GST; **e**, **k**), and glucose-6-phosphate dehydrogenase (G6PDH; **f**, **l**) activities in cerebral cortex and striatum of 30-day-old rats. Animals were euthanized 2 h after AdoMet injection. Data are represented as mean ± SD for 5–6 independent experiments (animals) performed in triplicate. $*P \leq 0.05$, $**P \leq 0.01$, $***P \leq 0.001$, compared to controls (Student's *t* test for unpaired samples)

0.0064] induced by AdoMet, while only NAC prevented GPx activity decrease (Fig. 7c) [(c): $F_{(3,16)} = 18.89$, $P < 0.0001$]. No effects were observed in sulfhydryl content (Fig. 7a), and CAT (Fig. 7e) and GST (Fig. 7f) activities.

AdoMet Intracerebral Administration Does Not Change Heme Oxygenase-1 Levels

Considering that heme oxygenase-1 (HO-1) is an antioxidant enzyme whose expression is modulated during oxidative stress [34], we measured the levels of this enzyme in both cerebral structures. Figure 8 shows no changes in the content of this enzyme 24 h after AdoMet injection.

AdoMet Intracerebral Administration Increases Iba1 Staining

We used immunofluorescence to evaluate protein Iba1, which is expressed at high levels by microglia during inflammatory processes [35]. Cerebral cortex sections (ventricular and subventricular layers of the neocortex) of animals injected with AdoMet showed marked increase of Iba1 staining

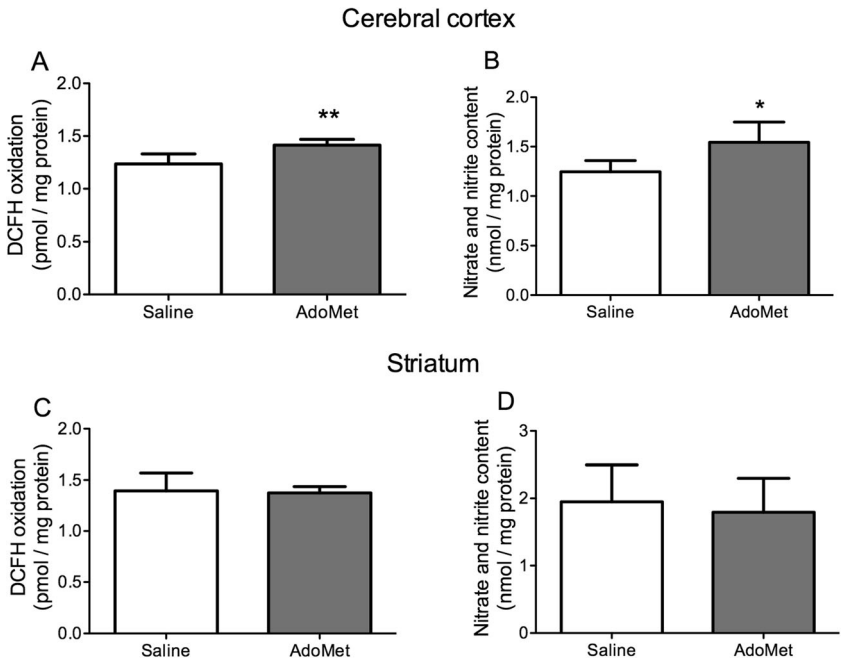

Fig. 4 Effect of S-adenosylmethionine (AdoMet) intracerebroventricular administration on 2′,7′-dichlorofluorescein (DCFH) oxidation (**a**, **c**) and nitrate and nitrite content (**b**, **d**) in cerebral cortex and striatum of 30-day-old rats. Animals were euthanized 2 h after AdoMet injection. Data are represented as mean ± SD for 5–6 independent experiments (animals) performed in triplicate. $*P \leq 0.05$, $**P \leq 0.01$, compared to controls (Student's *t* test for unpaired samples)

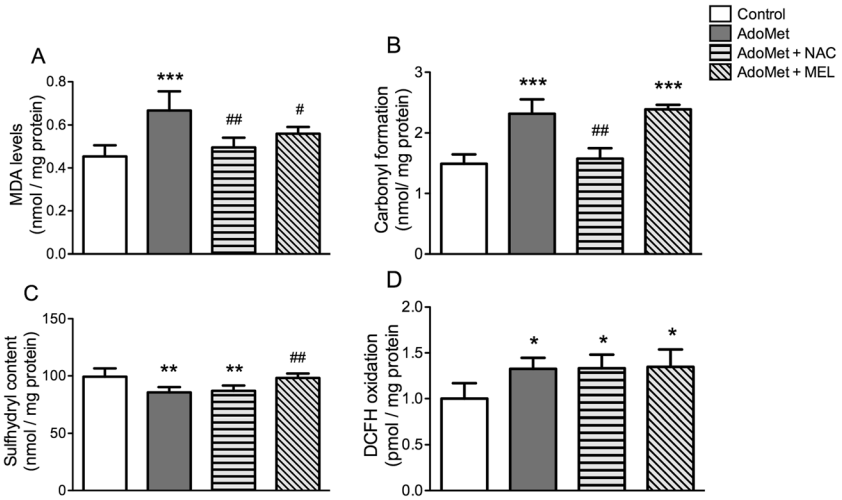

Fig. 5 Effect of N-acetylcysteine (NAC) and melatonin (MEL) on S-adenosylmethionine (AdoMet)-induced alterations of malondialdehyde (MDA) levels (**a**), carbonyl formation (**b**), sulfhydryl content (**c**), and 2′,7′-dichlorofluorescein (DCFH) oxidation (**d**) in cerebral cortex of 30-old-day rats. Animals were euthanized 2 h after AdoMet injection. Data are represented as mean ± SD for 5–6 independent experiments (animals) performed in triplicate. $^{*}P \leq 0.05$, $^{**}P \leq 0.01$, $^{***}P \leq 0.001$ compared to controls; $^{\#}P \leq 0.05$, $^{\#\#}P \leq 0.01$, compared to AdoMet group (Tukey's multiple range test)

compared to control (Fig. 9a) 5 days after administration, whereas no alterations were observed in the striatum sections (Fig. 9b) [(c): $t_{(4)} = 6.208$, $P = 0.0034$].

AdoMet Intracerebral Administration Decreases Synaptophysin Levels and Increases TAU Phosphorylation

We finally investigated the effects of AdoMet administration on the levels of synaptophysin protein, a membrane protein of pre-synaptic vesicles, and on TAU phosphorylation, a microtubule-associated protein, in rat cerebral cortex and striatum (Fig. 10). AdoMet significantly decreased synaptophysin levels [(a): $t_{(4)} = 3.489$, $P = 0.0126$] and increased TAU phosphorylation [(b): $t_{(4)} = 3.489$, $P = 0.0468$] in the cerebral cortex 24 h after its injection.

Discussion

Patients diagnosed with AdoHcy hydrolase deficiency predominantly accumulate AdoMet and present severe neurological dysfunction, including epilepsy and cortical atrophy [8], whose pathophysiology is still poorly known. In a previous work, we showed that exposing brain supernatants to AdoMet resulted in alterations of some parameters of oxidative stress

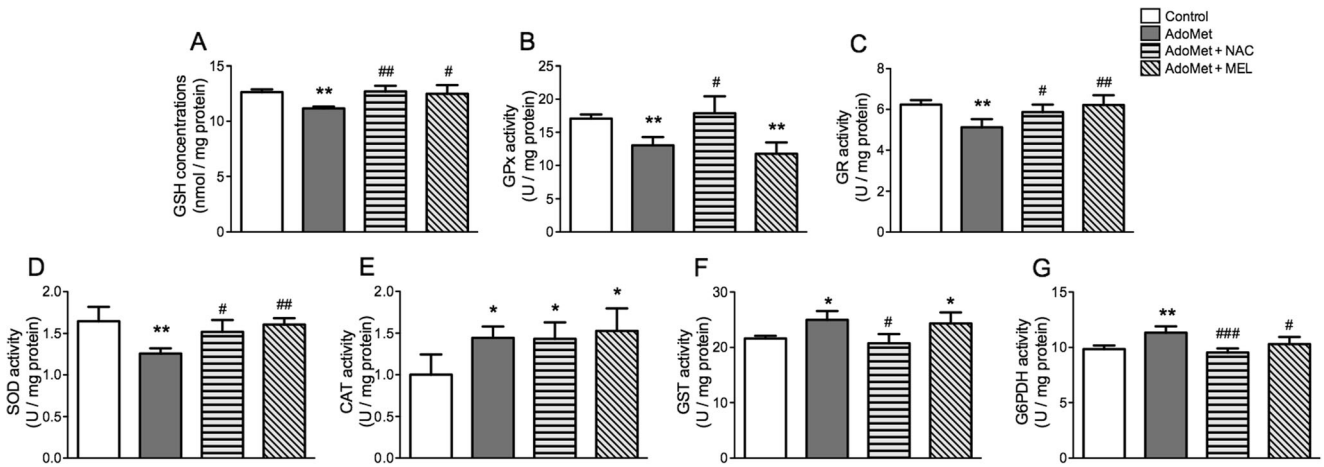

Fig. 6 Effect of N-acetylcysteine (NAC) and melatonin (MEL) on S-adenosylmethionine (AdoMet) alterations in reduced glutathione (GSH) concentrations (**a**), glutathione peroxidase (GPx; **b**), glutathione reductase (GR; **c**), superoxide dismutase (SOD; **d**), catalase (CAT; **e**), glutathione S-transferase (GST; **f**), and glucose-6-phosphate dehydrogenase (G6PDH; **g**) activities in cerebral cortex of 30-old-day rats. Animals were euthanized 2 h after AdoMet injection. Data are represented as mean ± SD for 5–6 independent experiments (animals) performed in triplicate. $^{*}P \leq 0.05$, $^{**}P \leq 0.01$, compared to controls; $^{\#}P \leq 0.05$, $^{\#\#}P \leq 0.01$, $^{\#\#\#}P \leq 0.001$, compared to AdoMet group (Tukey's multiple range test)

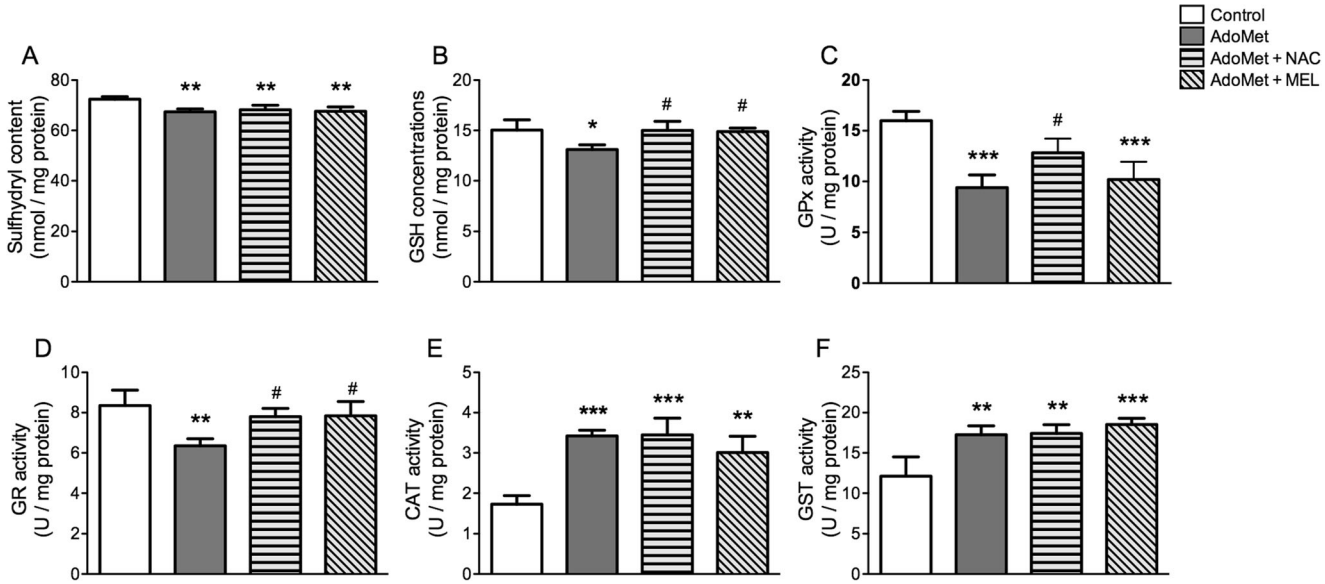

Fig. 7 Effect of N-acetylcysteine (NAC) and melatonin (MEL) on S-adenosylmethionine (AdoMet) alterations on sulfhydryl content (**a**), reduced glutathione (GSH) concentrations (**b**), glutathione peroxidase (GPx; **c**), glutathione reductase (GR; **d**), catalase (CAT; **e**), and glutathione S-transferase (GST; **f**) activities in striatum of 30-old-day rats. Animals were euthanized 2 h after AdoMet injection. Data are represented as mean ± SD for 5–6 independent experiments (animals) performed in triplicate. $^{*}P \leq 0.05$, $^{**}P \leq 0.01$, $^{***}P \leq 0.01$, compared to controls; $^{\#}P \leq 0.05$, compared to AdoMet group (Tukey's multiple range test)

in vitro [15]. In the present investigation, we extended these studies by evaluating whether high intracerebral concentrations of AdoMet induced by ICV administration of this compound could be toxic to the brain of developing rats. We measured a much larger spectrum of parameters of redox homeostasis, as well as microglia activation and the levels of neuronal proteins in rat cerebral cortex and striatum. We also tested the effects of classic antioxidants on the deleterious effects observed underlying AdoMet-elicited brain toxicity.

AdoMet administration induced biomolecule oxidative damage in cerebral cortex and striatum. We first verified that this metabolite increased the levels of MDA, an end product of membrane polyunsaturated fatty acid peroxidation, supporting previous in vitro findings [15]. AdoMet also induced protein oxidative damage, as observed by increased carbonyl formation and decreased sulfhydryl group content (increased sulfhydryl oxidation). In this context, it should be noted that carbonyl groups are mainly formed by oxidation of protein side chains, oxidative

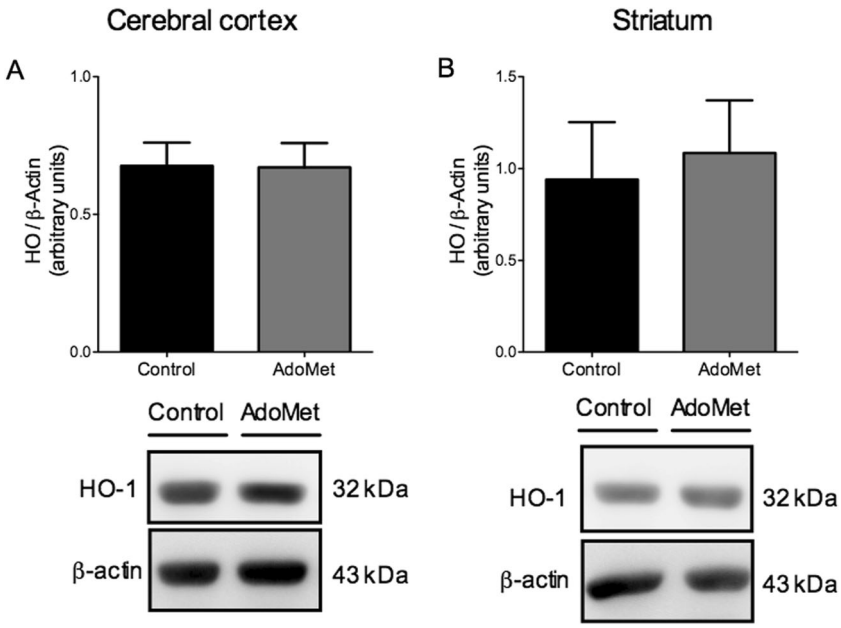

Fig. 8 Effect of S-adenosylmethionine (AdoMet) intracerebroventricular administration on the heme oxygenase-1 (HO-1) levels in cerebral cortex (**a**) and striatum (**b**) of young rats. Rats were euthanized 24 h after AdoMet injection. Representative immunoblots are shown as mean ± SD for three independent experiments (animals) normalized by β-actin levels. $^{*}P < 0.05$, compared to control (Student's *t* test for unpaired samples)

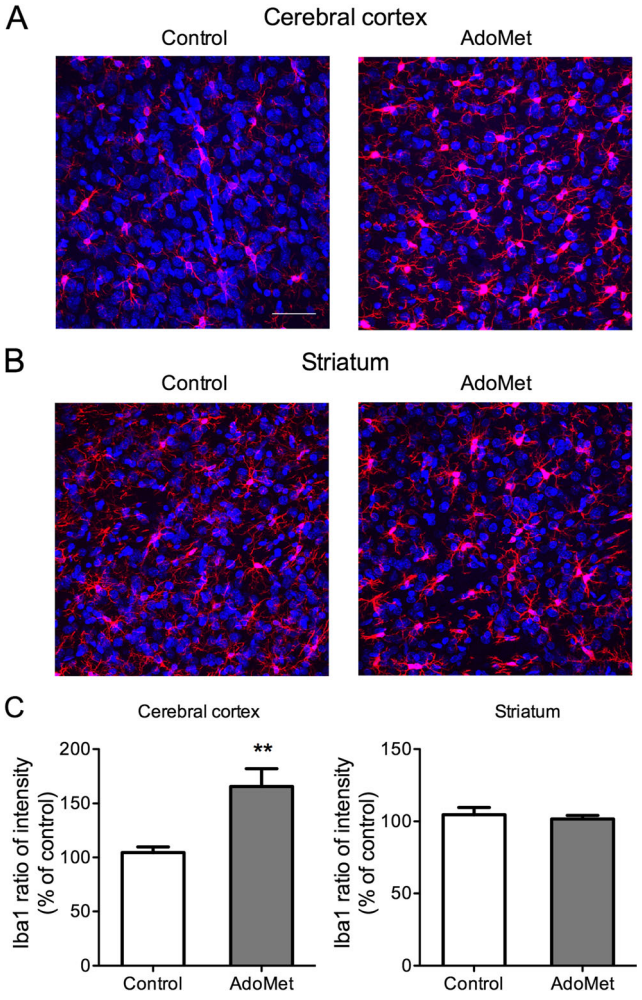

Fig. 9 Effect of S-adenosylmethionine (AdoMet) intracerebroventricular administration on Iba1 staining in cerebral cortex (**a**) and striatum (**b**) of 30-day-old rats. Animals were euthanized 5 days after AdoMet injection. Representative images of Iba1 immunofluorescence staining in rat cerebral cortex and striatum. Calibration bar indicates 200 μm. Quantification of Iba1 staining in rat cerebral cortex and striatum (**c**). Data are represented as mean ± SD for three independent experiments (animals) performed in triplicate and expressed as percentage of controls. $^{**}P \leq 0.01$, compared to control (Student's *t* test for unpaired samples)

cleavage of proteins, or by the reaction of reducing sugars with lysine protein residues [36]. Concerning the sulfhydryl content, since most sulfhydryl groups are protein-bound, it has been suggested that oxidation of these groups may lead to protein inactivation [22, 37].

Furthermore, AdoMet-induced lipid oxidative damage in cerebral cortex was totally prevented by the free radical scavengers NAC and MEL, suggesting that this effect was secondary to elevated reactive species generation, mainly hydroxyl and peroxyl radicals, and peroxynitrite, which are scavenged by these antioxidants [14, 38–40]. On the other hand, only NAC was able to prevent the increase of carbonyl formation, while MEL prevented the decrease of sulfhydryl content induced by AdoMet in cerebral cortex.

The cerebral cortex and striatum nonenzymatic antioxidant defenses were also compromised by AdoMet, as verified by the decrease of tGS and GSH, as well as increase of GSSG concentrations. This antioxidant is considered an indicator of the nonenzymatic antioxidant capacity of a tissue to prevent the damage associated with free radical processes [14]. Moreover, since GSH is a crucial brain defense against oxidative damage by acting as a reactive species scavenger and as a cofactor for enzymes that remove free radicals, it is feasible that the decrease of this important antioxidant could make lipids and proteins more vulnerable to AdoMet-induced oxidative damage. In this scenario, it was also observed that the decrease of GSH concentrations was also abolished by NAC and MEL, similarly to what was found in AdoMet-induced lipid and protein oxidative damage.

Regarding the enzymatic antioxidant defenses, we verified that AdoMet significantly decreased GPx, GR, and SOD activities, and increased CAT, GST, and G6PDH activities. Although we cannot at present determine the mechanisms by which GPx, GR, and SOD activities were reduced, it has been suggested that a decrease in the activity of antioxidant enzymes may be due to reactive species causing a site-specific amino acid modification [41]. On the other hand, it is feasible that the increase of CAT, GST, and G6PDH activities induced by AdoMet could be related to upregulation of these enzymes at the gene level that might have occurred as a compensatory mechanism in response to increased formation of reactive species [14, 42, 43]. In this regard, we found that the levels of HO-1, an antioxidant enzyme classically modulated by Nrf2 pathway [34], were not modified by AdoMet, suggesting that other signaling pathways are possibly involved in the upregulation of CAT, GST, and G6PDH induced by AdoMet.

We also showed that AdoMet increased ROS generation, as reflected by DCFH oxidation increase, corroborating previous data showing that AdoMet increased hydrogen peroxide production in vitro in rat brain mitochondrial preparations [15]. Since DCFH is converted to DCF mainly by hydrogen peroxide and hydroxyl radicals [44, 45], this result reinforces our assumption that these ROS were probably involved in AdoMet pro-oxidant effects, as previously suggested. Furthermore, AdoMet increased nitrate and nitrite levels, indicating that RNS formation also underlies the pro-oxidant effects on biomolecules elicited by this metabolite. In this particular, it is well known that peroxynitrite is capable of initiating lipid peroxidation cascade and may lead to severe cell membrane damage [14].

Another novel finding of the present work was that AdoMet increased the staining of Iba1, considered an excellent marker of microglia activation. Since uncontrolled activation of microglia can lead to excessive production of pro-inflammatory cytokines and free radicals [46–50], it may be suggested that AdoMet is a toxic metabolite with potential to induce neuroinflammation. This is reinforced by the fact that

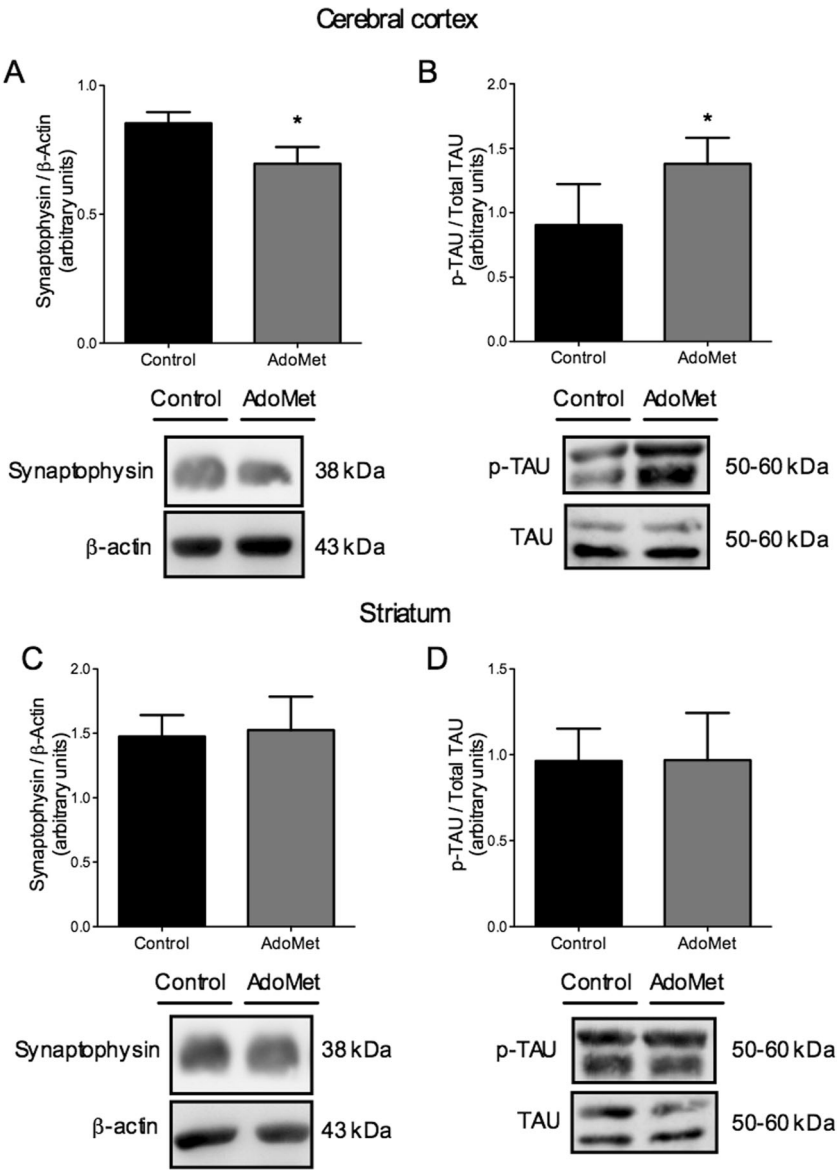

Fig. 10 Effect of S-adenosylmethionine (AdoMet) intracerebroventricular administration on the synaptophysin levels and Tau protein phosphorylation in cerebral cortex (**a**, **b**, respectively) and striatum (**c**, **d**, respectively) of young rats. Rats were euthanized 24 h after AdoMet injection. Representative immunoblots are shown as mean ± SD for three independent experiments (animals) normalized by β-actin levels. $^{*}P < 0.05$, compared to control (Student's *t* test for unpaired samples)

AdoMet increased nitrate and nitrite content, implying activation of inducible nitric oxide synthase (iNOS). Of note, it is known that activation of toll-like receptors in microglia and also in astrocytes leads to excessive production of nitric oxide via iNOS [51].

Additionally, AdoMet administration decreased the levels of synaptophysin in cerebral cortex. Synaptophysin is an abundant integral membrane protein of pre-synaptic vesicles essential for the formation and maintenance of synapses, regulation of neurotransmitter release, and synaptic plasticity, so that the decrease of this protein probably reflects axonal damage [52, 53]. This is in accordance with other studies showing that synaptophysin is downregulated in response to stress conditions, leading to impairment of synaptic integrity [54, 55]. AdoMet also increased the phosphorylation of TAU, a microtubule-associated protein involved in the outgrowth of neural processes, axonal transport, development of neuronal polarity, and maintenance of normal neuron morphology [56, 57]. Deregulated TAU phosphorylation may result in abnormal neuronal dysfunction and lead to neuronal loss [58, 59]. Taken together these data, it is presumed that alterations in synaptophysin levels and TAU phosphorylation may be involved in the neurological dysfunction of AdoHcy hydrolase deficiency.

Our study shows, for the first time, that AdoMet provokes oxidative stress and induces microglia activation and neuronal damage in cerebral cortex and striatum of rats. It is postulated that these pathological mechanisms may be possibly involved in the onset and progression of the neurologic symptoms and abnormalities in AdoHcy hydrolase deficiency. On the other hand, although we cannot establish whether microglia activation is the primary causative event or a consequence of

oxidative stress, it is conceivable that the activation of these neural cells may also participate in the neuropathology of AdoHcy hydrolase deficiency.

Conclusion

In conclusion, the present investigation showed that AdoMet markedly disturbs redox homeostasis and induces microglia activation, besides provoking synapse and neuron microtubule alterations in brain of young rats. In case oxidative stress is found in tissues (blood, fibroblasts, and skeletal muscle) from patients affected by AdoHcy hydrolase deficiency, it could be presumed that disturbance of redox cell status and microglia activation contribute at least in part to the pathophysiology of the cerebral abnormalities observed in patients affected by this disorder. Moreover, since oxidative and nitrosative stress may possibly play a role in its pathogenesis, replenishment of intracellular GSH by NAC or the administration of MEL or other antioxidant could be beneficial as adjuvant therapies. Finally, investigation of the effects of AdoMet on other parameters of neuronal function, besides synaptophysin expression and TAU phosphorylation, seems necessary to better clarify whether neuronal integrity could be compromised by this metabolite.

Funding Information This work was supported by the Conselho Nacional de Desenvolvimento Científico e Tecnológico [grant number #404883/2013-3], Fundação de Amparo à Pesquisa do Estado do Rio Grande do Sul [grant number #2266- 2551/14-2], and Financiadora de Estudos e Projetos/Rede Instituto Brasileiro de Neurociência [grant number #01.06.0842-00].

Compliance with Ethical Standards

The experimental protocol was approved by the local Animal Ethics Committe of Universidade Federal do Rio Grande do Sul. The guidelines of National Institutes of Health Guide for the Care and Use of Laboratory Animals (NIH publication no. 80–23, revised 2011) and Directive 2010/63/EU were followed.

Conflict of Interest The authors declare that they have no conflicts of interest.

References

1. Gaull GE, Von Berg W, Raiha NC, Sturman JA (1973) Development of methyltransferase activities of human fetal tissues. Pediatr Res 7(5):527–533. https://doi.org/10.1203/00006450-197305000-00006
2. Grubbs R, Vugrek O, Deisch J, Wagner C, Stabler S, Allen R, Baric I, Rados M et al (2010) S-adenosylhomocysteine hydrolase deficiency: two siblings with fetal hydrops and fatal outcomes. J Inherit Metab Dis 33(6):705–713. https://doi.org/10.1007/s10545-010-9171-x
3. Honzik T, Magner M, Krijt J, Sokolova J, Vugrek O, Beluzic R, Baric I, Hansikova H et al (2012) Clinical picture of S-adenosylhomocysteine hydrolase deficiency resembles phosphomannomutase 2 deficiency. Mol Genet Metab 107(3):611–613. https://doi.org/10.1016/j.ymgme.2012.08.014
4. Mudd SH, Brosnan JT, Brosnan ME, Jacobs RL, Stabler SP, Allen RH, Vance DE, Wagner C (2007) Methyl balance and transmethylation fluxes in humans. Am J Clin Nutr 85(1):19–25. https://doi.org/10.1093/ajcn/85.1.19
5. Stender S, Chakrabarti RS, Xing C, Gotway G, Cohen JC, Hobbs HH (2015) Adult-onset liver disease and hepatocellular carcinoma in S-adenosylhomocysteine hydrolase deficiency. Mol Genet Metab 116(4):269–274. https://doi.org/10.1016/j.ymgme.2015.10.009
6. Strauss KA, Ferreira C, Bottiglieri T, Zhao X, Arning E, Zhang S, Zeisel SH, Escolar ML et al (2015) Liver transplantation for treatment of severe S-adenosylhomocysteine hydrolase deficiency. Mol Genet Metab 116(1–2):44–52. https://doi.org/10.1016/j.ymgme.2015.06.005
7. Baric I, Staufner C, Augoustides-Savvopoulou P, Chien YH, Dobbelaere D, Grunert SC, Opladen T, Petkovic Ramadza D et al (2017) Consensus recommendations for the diagnosis, treatment and follow-up of inherited methylation disorders. J Inherit Metab Dis 40(1):5–20. https://doi.org/10.1007/s10545-016-9972-7
8. Baric I, Fumic K, Glenn B, Cuk M, Schulze A, Finkelstein JD, James SJ, Mejaski-Bosnjak V et al (2004) S-adenosylhomocysteine hydrolase deficiency in a human: a genetic disorder of methionine metabolism. Proc Natl Acad Sci U S A 101(12):4234–4239. https://doi.org/10.1073/pnas.0400658101
9. Baric I, Cuk M, Fumic K, Vugrek O, Allen RH, Glenn B, Maradin M, Pazanin L et al (2005) S-Adenosylhomocysteine hydrolase deficiency: a second patient, the younger brother of the index patient, and outcomes during therapy. J Inherit Metab Dis 28(6):885–902. https://doi.org/10.1007/s10545-005-0192-9
10. Finkelstein JD, Kyle W, Harris BJ (1971) Methionine metabolism in mammals. Regulation of homocysteine methyltransferases in rat tissue. Arch Biochem Biophys 146(1):84–92
11. Gao J, Cahill CM, Huang X, Roffman JL, Lamon-Fava S, Fava M, Mischoulon D, Rogers JT (2018) S-Adenosyl methionine and transmethylation pathways in neuropsychiatric diseases throughout life. Neurotherapeutics 15(1):156–175. https://doi.org/10.1007/s13311-017-0593-0
12. Rubin RA, Ordonez LA, Wurtman RJ (1974) Physiological dependence of brain methionine and S-adenosylmethionine concentrations on serum amino acid pattern. J Neurochem 23(1):227–231
13. Molloy AM, Orsi B, Kennedy DG, Kennedy S, Weir DG, Scott JM (1992) The relationship between the activity of methionine synthase and the ratio of S-adenosylmethionine to S-adenosylhomocysteine in the brain and other tissues of the pig. Biochem Pharmacol 44(7):1349–1355
14. Halliwell BGJ (2015) Cellular responses to oxidative stress: adaptation, damage, repair, senescence and death. In: Free radicals in biology and medicine. Oxford University Press Inc, Oxford, pp. 199–283
15. Zanatta A, Cecatto C, Ribeiro RT, Amaral AU, Wyse AT, Leipnitz G, Wajner M (2017) S-Adenosylmethionine promotes oxidative stress and decreases Na(+), K(+)-ATPase activity in cerebral cortex supernatants of adolescent rats: implications for the pathogenesis of S-adenosylhomocysteine hydrolase deficiency. Mol Neurobiol 55:5868–5878. https://doi.org/10.1007/s12035-017-0804-z
16. Paxinos G, Watson C (2013) The rat brain in stereotaxic coordinates, 7th edn. Academic, Cambridge
17. da Rosa MS, Joao Ribeiro CA, Seminotti B, Teixeira Ribeiro R, Amaral AU, Coelho Dde M, de Oliveira FH, Leipnitz G et al (2015) In vivo intracerebral administration of L-2-hydroxyglutaric acid provokes oxidative stress and histopathological alterations in

striatum and cerebellum of adolescent rats. Free Radic Biol Med 83: 201–213. https://doi.org/10.1016/j.freeradbiomed.2015.02.008
18. Evelson P, Travacio M, Repetto M, Escobar J, Llesuy S, Lissi EA (2001) Evaluation of total reactive antioxidant potential (TRAP) of tissue homogenates and their cytosols. Arch Biochem Biophys 388(2):261–266. https://doi.org/10.1006/abbi.2001.2292
19. Lowry OH, Rosebrough NJ, Farr AL, Randall RJ (1951) Protein measurement with the Folin phenol reagent. J Biol Chem 193(1): 265–275
20. Yagi K (1998) Simple procedure for specific assay of lipid hydroperoxides in serum or plasma. Methods Mol Biol 108:107–110. https://doi.org/10.1385/0-89603-472-0:107
21. Reznick AZ, Packer L (1994) Oxidative damage to proteins: spectrophotometric method for carbonyl assay. Methods Enzymol 233: 357–363
22. Aksenov MY, Markesbery WR (2001) Changes in thiol content and expression of glutathione redox system genes in the hippocampus and cerebellum in Alzheimer's disease. Neurosci Lett 302(2–3): 141–145
23. Browne RW, Armstrong D (1998) Reduced glutathione and glutathione disulfide. Methods Mol Biol 108:347–352. https://doi.org/10.1385/0-89603-472-0:347
24. Teare JP, Punchard NA, Powell JJ, Lumb PJ, Mitchell WD, Thompson RP (1993) Automated spectrophotometric method for determining oxidized and reduced glutathione in liver. Clin Chem 39(4):686–689
25. Wendel A (1981) Glutathione peroxidase. Methods Enzymol 77: 325–333
26. Carlberg I, Mannervik B (1985) Glutathione reductase. Methods Enzymol 113:484–490
27. Marklund SL (1985) Product of extracellular-superoxide dismutase catalysis. FEBS Lett 184(2):237–239
28. Aebi H (1984) Catalase in vitro. Methods Enzymol 105:121–126
29. Guthenberg C, Mannervik B (1981) Glutathione S-transferase (transferase pi) from human placenta is identical or closely related to glutathione S-transferase (transferase rho) from erythrocytes. Biochim Biophys Acta 661(2):255–260
30. Leong SF, Clark JB (1984) Regional development of glutamate dehydrogenase in the rat brain. J Neurochem 43(1):106–111
31. LeBel CP, Ischiropoulos H, Bondy SC (1992) Evaluation of the probe 2′,7′-dichlorofluorescin as an indicator of reactive oxygen species formation and oxidative stress. Chem Res Toxicol 5(2): 227–231
32. Navarro-Gonzalvez JA, Garcia-Benayas C, Arenas J (1998) Semiautomated measurement of nitrate in biological fluids. Clin Chem 44(3):679–681
33. Moura AP, Parmeggiani B, Gasparotto J, Grings M, Fernandez Cardoso GM, Seminotti B, Moreira JCF, Gelain DP et al (2018) Glycine administration alters MAPK signaling pathways and causes neuronal damage in rat brain: putative mechanisms involved in the neurological dysfunction in nonketotic hyperglycinemia. Mol Neurobiol 55(1):741–750. https://doi.org/10.1007/s12035-016-0319-z
34. Waza AA, Hamid Z, Ali S, Bhat SA, Bhat MA (2018) A review on heme oxygenase-1 induction: is it a necessary evil. Inflamm Res 67: 579–588. https://doi.org/10.1007/s00011-018-1151-x
35. Hoogland IC, Houbolt C, van Westerloo DJ, van Gool WA, van de Beek D (2015) Systemic inflammation and microglial activation: systematic review of animal experiments. J Neuroinflammation 12: 114. https://doi.org/10.1186/s12974-015-0332-6
36. Dalle-Donne I, Rossi R, Giustarini D, Milzani A, Colombo R (2003) Protein carbonyl groups as biomarkers of oxidative stress. Clin Chim Acta 329(1–2):23–38
37. Davies MJ (2003) Singlet oxygen-mediated damage to proteins and its consequences. Biochem Biophys Res Commun 305(3):761–770
38. Reiter RJ, Tan DX, Manchester LC, Qi W (2001) Biochemical reactivity of melatonin with reactive oxygen and nitrogen species: a review of the evidence. Cell Biochem Biophys 34(2):237–256. https://doi.org/10.1385/CBB:34:2:237
39. Anisimov VN (2006) Premature ageing prevention: limitations and perspectives of pharmacological interventions. Curr Drug Targets 7(11):1485–1503
40. Elbini Dhouib I, Jallouli M, Annabi A, Gharbi N, Elfazaa S, Lasram MM (2016) A minireview on N-acetylcysteine: an old drug with new approaches. Life Sci 151:359–363. https://doi.org/10.1016/j.lfs.2016.03.003
41. Singh P, Jain A, Kaur G (2004) Impact of hypoglycemia and diabetes on CNS: correlation of mitochondrial oxidative stress with DNA damage. Mol Cell Biochem 260(1–2):153–159
42. Kaushik S, Kaur J (2003) Chronic cold exposure affects the antioxidant defense system in various rat tissues. Clin Chim Acta 333(1):69–77
43. Jafari M (2007) Dose- and time-dependent effects of sulfur mustard on antioxidant system in liver and brain of rat. Toxicology 231(1): 30–39. https://doi.org/10.1016/j.tox.2006.11.048
44. Myhre O, Andersen JM, Aarnes H, Fonnum F (2003) Evaluation of the probes 2′,7′-dichlorofluorescin diacetate, luminol, and lucigenin as indicators of reactive species formation. Biochem Pharmacol 65(10):1575–1582
45. Bonini MG, Rota C, Tomasi A, Mason RP (2006) The oxidation of 2′,7′-dichlorofluorescin to reactive oxygen species: a self-fulfilling prophesy? Free Radic Biol Med 40(6):968–975. https://doi.org/10.1016/j.freeradbiomed.2005.10.042
46. Ito D, Imai Y, Ohsawa K, Nakajima K, Fukuuchi Y, Kohsaka S (1998) Microglia-specific localisation of a novel calcium binding protein, Iba1. Brain Res Mol Brain Res 57(1):1–9
47. Serrano-Pozo A, Gomez-Isla T, Growdon JH, Frosch MP, Hyman BT (2013) A phenotypic change but not proliferation underlies glial responses in Alzheimer disease. Am J Pathol 182(6):2332–2344. https://doi.org/10.1016/j.ajpath.2013.02.031
48. Wirths O, Breyhan H, Marcello A, Cotel MC, Bruck W, Bayer TA (2010) Inflammatory changes are tightly associated with neurodegeneration in the brain and spinal cord of the APP/PS1KI mouse model of Alzheimer's disease. Neurobiol Aging 31(5):747–757. https://doi.org/10.1016/j.neurobiolaging.2008.06.011
49. Norden DM, Trojanowski PJ, Villanueva E, Navarro E, Godbout JP (2016) Sequential activation of microglia and astrocyte cytokine expression precedes increased Iba-1 or GFAP immunoreactivity following systemic immune challenge. Glia 64(2):300–316. https://doi.org/10.1002/glia.22930
50. Balducci C, Forloni G (2018) Novel targets in Alzheimer's disease: a special focus on microglia. Pharmacol Res 130:402–413. https://doi.org/10.1016/j.phrs.2018.01.017
51. Sun L, Shen R, Agnihotri SK, Chen Y, Huang Z, Bueler H (2018) Lack of PINK1 alters glia innate immune responses and enhances inflammation-induced, nitric oxide-mediated neuron death. Sci Rep 8(1):383. https://doi.org/10.1038/s41598-017-18786-w
52. Gudi V, Gai L, Herder V, Tejedor LS, Kipp M, Amor S, Suhs KW, Hansmann F et al (2017) Synaptophysin is a reliable marker for axonal damage. J Neuropathol Exp Neurol 76:109–125. https://doi.org/10.1093/jnen/nlw114
53. Wang X, Cheng JL, Ran YC, Zhang Y, Yang L, Lin YN (2017) Expression of RGMb in brain tissue of MCAO rats and its relationship with axonal regeneration. J Neurol Sci 383:79–86. https://doi.org/10.1016/j.jns.2017.10.032
54. Thome J, Pesold B, Baader M, Hu M, Gewirtz JC, Duman RS, Henn FA (2001) Stress differentially regulates synaptophysin and synaptotagmin expression in hippocampus. Biol Psychiatry 50(10): 809–812
55. Xu H, He J, Richardson JS, Li XM (2004) The response of synaptophysin and microtubule-associated protein 1 to restraint

stress in rat hippocampus and its modulation by venlafaxine. J Neurochem 91(6):1380–1388. https://doi.org/10.1111/j.1471-4159.2004.02827.x

56. Terry RD (1998) The cytoskeleton in Alzheimer disease. J Neural Transm Suppl 53:141–145
57. Kuszczyk M, Gordon-Krajcer W, Lazarewicz JW (2009) Homocysteine-induced acute excitotoxicity in cerebellar granule cells in vitro is accompanied by PP2A-mediated dephosphorylation of tau. Neurochem Int 55(1–3):174–180. https://doi.org/10.1016/j.neuint.2009.02.010
58. Abisambra JF, Jinwal UK, Blair LJ, O'Leary JC 3rd, Li Q, Brady S, Wang L, Guidi CE et al (2013) Tau accumulation activates the unfolded protein response by impairing endoplasmic reticulum-associated degradation. J Neurosci 33(22):9498–9507. https://doi.org/10.1523/JNEUROSCI.5397-12.2013
59. Lee VM, Goedert M, Trojanowski JQ (2001) Neurodegenerative tauopathies. Annu Rev Neurosci 24:1121–1159. https://doi.org/10.1146/annurev.neuro.24.1.1121